Assessing the applicability of the Actuaries Climate Index within a weather derivatives framework

José Garrido

Concordia University, Montreal, Canada jose.garrido@concordia.ca

Actuarial Research Conference York University, Toronto, July 29–August 1, 2025

https://arxiv.org/abs/2504.21143

Research funded by the Natural Sciences and Engineering Research Council of Canada (NSERC)



July 29 - August 1, 2025

Collaborators



A. Sevtap Selcuk-Kestel



Cem Yavrum

Institute of Applied Mathematics, METU, Ankara, Turkey



In memoriam: Ricardas Zitikis (1962–2025)



Yi Lu's PhD thesis defence, March 11, 2005



Outline

- Introduction
- Weather-based indexes and ACI
- Methodology
 - First stage
 - Second stage
- 4 Empirical Analysis
- Conclusions
- 6 References



July 29 - August 1, 2025

Introduction – I

- As the effects of climate change become more severe, an increasing number of sectors, including agriculture, insurance, energy, and tourism, become more vulnerable to weather related risks.
- These industries have the option to use weather derivatives as a tool to manage or reduce these risks.
- Weather derivatives are financial instruments to hedge against adverse weather conditions, with their value contingent upon specific weather variables.
- Products based on index values, such as CDD and HDD that vary according to temperature, are already available on the Chicago Mercantile Exchange (see CME Group, 2024).
- In 2016, the Actuaries Climate Index[™] (ACI) was launched by four major North American actuarial societies, using climate data from the US and Canada, see [1].

Introduction - II

- The ACI includes 6 climate variables and indicates extreme weather conditions for 12 subregions across the US and Canada: high and low temperatures, precipitation, drought, wind, and sea level.
- It is designed as a monitoring tool for insurance companies, policymakers, and individuals to track weather changes and the associated risks.



Aim of the study

- This study compares the Actuaries Climate IndexTM, with long-established weather-based indexes commonly used in energy and derivatives markets, through regression models: generalized linear model (GLM), generalized additive model (GAM), and machine learning algorithms: extreme gradient boosting (XGB) and light gradient boosting machine (LGBM).
- Beyond comparing the predictive power of the indexes, we investigate
 the individual contribution of each weather index to model
 performance by fitting 22 distinct models, built with different
 explanatory variables.
- All explanatory variables are weather-based; they may share common weather driven patterns. To address the potential multicollinearity we apply dimension reduction techniques: principal component analysis (PCA) and functional principal component analysis (FPCA).

Weather-based indexes (CDD, HDD), see [5]

Temperature: Let T_i^{max} and T_i^{min} denote the maximum and minimum air temperatures observed on day i. These are averaged :

$$T_i = \frac{T_i^{\text{max}} + T_i^{\text{min}}}{2}.$$
 (1)

Then, the cooling degree–days (CDD), and heating degree–days (HDD) generated on that day are defined as the excess air temperature over a threshold (usually 65° F or 18° C):

$$CDD_i = max\{T_i - 65, 0\}, \tag{2}$$

$$HDD_i = max\{65 - T_i, 0\}.$$
 (3)



8 / 28

Weather-based indexes (PRE), see [10]

The cumulative rainfall index (PRE) is the daily or monthly aggregate rainfall (in mm), defined as:

$$PRE = \sum_{t=1}^{N} r_t, \tag{4}$$

where N denotes the accumulation period, and r_t is the rainfall observed for time t.



Actuaries Climate Index[™] (T90, T10, P)

- T90: % of days when day temperatures > the corresponding 90-th percentile of the reference period for the relevant days.
- T10: % of days when day temperatures < the corresponding 10-th percentile of the reference period for the relevant days.
- P: The maximum rainfall in any 5 consecutive days in the month.

ACI uses standardized values for all components, based on the values mean and standard deviation over the reference period, 1961–1990, [1]:

$$T90_{std}(j,k) = \frac{T90(j,k) - \mu_{ref}T90(j)}{\sigma_{ref}T90(j)},$$
 (5)

$$T10_{std}(j,k) = \frac{T10(j,k) - \mu_{ref} T10(j)}{\sigma_{ref} T10(j)},$$
 (6)

$$P_{std}(j,k) = \frac{Rx5day(j,k) - \mu_{ref}Rx5day(j)}{\sigma_{ref}Rx5day(j)},$$
(7)

where j is the month or season, k is the year, μ_{ref} and σ_{ref} are the component mean and standard deviation over the reference period.



Methodology

The analyses are conducted in two stages :

- The first stage seeks similarities between WBI and ACI components. We check how strongly correlated these two indexes are and define their empirical cumulative distribution functions.
- The second stage focuses on testing and comparing the predictive performance of climate indexes on crop yields. Crop yields are predicted using regression models and machine learning algorithms that comprise a total of 22 distinct models, each constructed with different explanatory variables.



Methodology (first stage)

- Indexes measuring similar weather conditions are grouped into categories such as warm weather, cool weather and precipitation to facilitate meaningful comparisons, as detailed in Table 1.
- The grouping structure is based on the specific meteorological conditions represented by each index.

Table 1: Structure of groups

Group	Weather–Based Indexes (WBI)	Components of the ACI	Season	Measurement
1	CDD	T90	Summer	Warm weather
2	HDD	T10	Winter	Cool weather
3	PRE	Р	Spring	Precipitation

- The Spearman rank correlation coefficient (see [16]).
- Kolmogorov-Smirnov (K-S) test (see [7]).



July 29 - August 1, 2025

Methodology (second stage)

- The predictive capabilities of climate indexes on the yields of corn, wheat, and soybeans are examined using traditional statistical methods (GLMs, see [8] or GAMs, see [13, 15]) and machine learning algorithms (XGB, see [2], and LGBM, see [6]).
- The analyses fit 22 models, each incorporating explanatory variables representing various weather measurements and their combinations.
- Table 2 gives a breakdown of each model and its associated data set.

Table 2: Explanatory variables included in predicting crop yields

Model	Explanatory	Model	Explanatory	Model	Explanatory
#	Variables	#	Variables	#	Variables
1	CDD	8	T90	15	T90-T10-P-W
2	HDD	9	T10	16	T90-T10-P-D
3	PRE	10	Р	17	T90-T10-P-S
4	CDD-HDD	11	T90-T10	18	T90-T10-P-W-D
5	CDD-PRE	12	T90-P	19	T90-T10-P-W-S
6	HDD-PRE	13	T10-P	20	T90-T10-P-D-S
7	CDD-HDD-PRE	14	T90-T10-P	21	T90-T10-P-W-D-S
		22	ACI		

Note: Based on four meteorological season values for each index.



Methodology (second stage)

- The choice of explanatory variables for each model follows a logical progression, designed to evaluate the predictive power of various index configurations on crop yields.
- In the first comparison analysis, the performance of regression models and machine learning algorithms is assessed using principal components derived from the explanatory variables.
- To ensure independence between explanatory variables, and simplify the analysis without compromising model accuracy, we use PCA (see [11, 4]) and FPCA (see [12]) as dimensionality reduction techniques.
- In the second comparison analysis, the climate indexes are directly used as input variables in the machine learning algorithms without applying any dimensionality reduction.



Methodology (second stage)

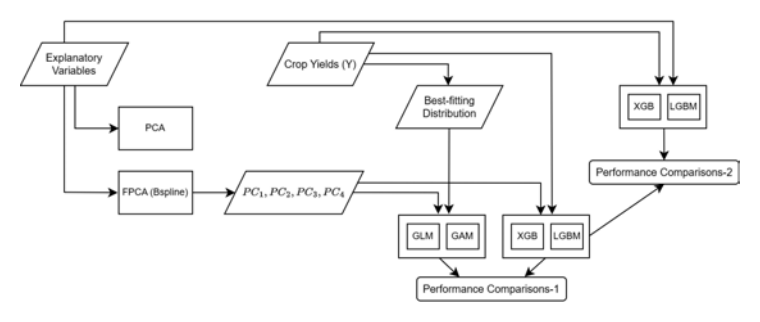


Figure 1: Flowchart of the proposed methodology

- From the transformed data, the first 4 principal components (PC_1 , PC_2 , PC_3 , PC_4), collectively account for more than 85% of the variance in the data and are selected as model input variables.
- The distribution of crop yield data is determined before conducting the regression analyses.

Data

- This study focuses specifically on U.S. data, where states are grouped into seven sub-regions (ALA, CEA, CWP, MID, SEA, SPL, SWP) based on their geographic locations. ACI values, from (see [1]), cover a 63-year period from 1961 to 2023 for each of the seven sub-regions.
- The National Oceanic and Atmospheric Administration (NOAA) (see [9]) provides monthly data on CDD, HDD, and PRE for all U.S. states (except ALA), covering the period from 1895 to the present.
- Annual yield data (in bushels per acre) for corn, wheat, and soybeans is obtained from the United States Department of Agriculture (USDA) (see [14]) for all states, covering the period from 1961 to 2023. For soybeans, the analysis is limited to 4 regions: CEA, CWP, MID and SEA, as yield data is only available for these areas.



July 29 - August 1, 2025

Results - I

Despite methodological differences in constructing the indexes, strong positive correlations are observed between the weather–based indexes and their corresponding components of the ACI.

Table 3: Similarity tests within each group

		Region							
		CEA	CWP	MID	SEA	SPL	SWP		
Group-1	r	0.88	0.90	0.89	0.94	0.86	0.96		
(CDD-T90)	K-S test (p)	0.089	< 0.01	< 0.01	< 0.01	< 0.01	0.408		
Group-2	r	0.89	0.83	0.86	0.87	0.81	0.79		
(HDD-T10)	K-S test (p)	0.011	< 0.01	< 0.01	0.019	0.204	0.055		
Group-3	r	0.83	0.81	0.87	0.87	0.68	0.85		
(PRE-P)	K-S test (p)	0.293	0.293	0.408	0.089	< 0.01	0.089		

Note: r-Spearman rank correlation coefficient.



Results - II

- In the second stage, the explanatory variables in each model are transformed into their principal components using PCA and FPCA.
- Figure 2 displays the total variation in the data sets, represented as regional averages, explained by the first four principal components derived from both methods for each model.

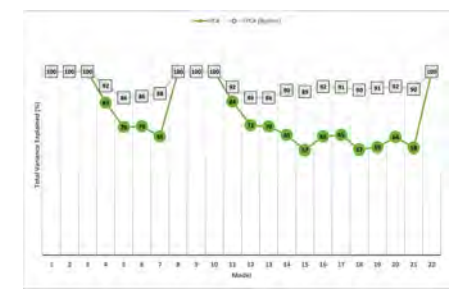


Figure 2: Explained variance comparisons, PCA vs FPCA as regional averages

Results - III

 Model 19 (T90, T10, P, W, S) with XGB yields the best performance with a pR² of 86.6% (train) and a MAPE of 14.3% (test).

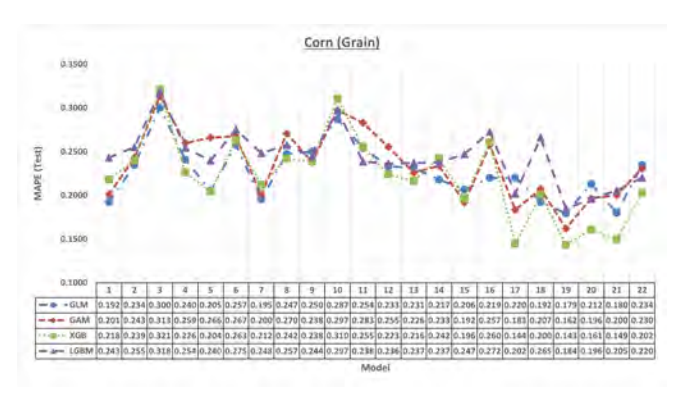


Figure 3: MAPE values (test) of each model as regional averages; Corn (grain)



Results - IV

 Model 19 (T90, T10, P, W, S) with GAM gives the best performance with a pR² of 61.9% (train) and a MAPE of 12.4% (test).

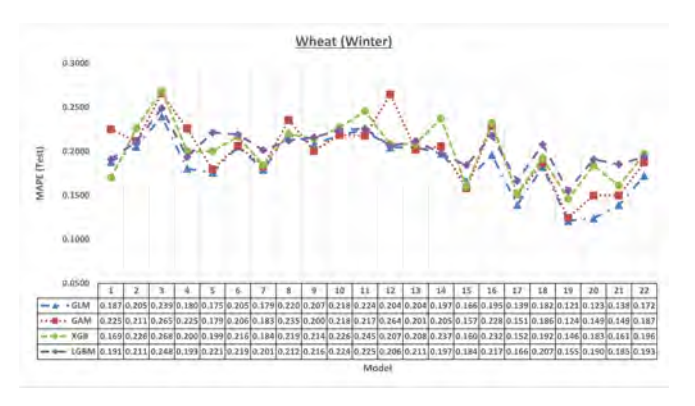


Figure 4: MAPE values (test) of each model as regional averages; Wheat (winter)



Results - V

 Model 17 (T90, T10, P, S) with GAM yields the best performance with a pR² of 72.1% (train) and a MAPE of 12.5% (test).

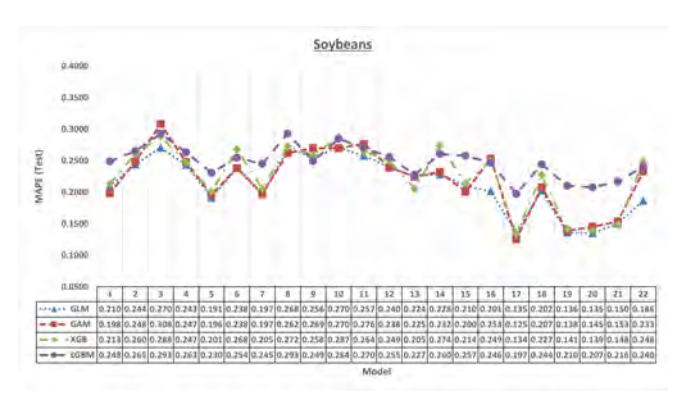


Figure 5: MAPE values (test) of each model as regional averages; Soybeans



Results - VI

- Notably, with the XGB-C method, Model 21 (which incorporates all 6 components of ACI and thus constitutes the largest data set) consistently yields the best performance.
- The second-best performing models remain consistent with those from the first comparison analysis (Model 19 for corn and wheat, Model 17 for soybeans).

(see Table 4 below)



Results - VII

Table 4: Performance comparison-2, as regional averages for each crop

		Corn (Grain)		Wheat (Winter)				Soybeans			
Model	el pR2 (Train)		MAPE (Test)		pR2 (Train)		MAPE (Test)		pR2 (Train)		MAPE (Test)	
	XGB	XGB-C	XGB	XGB-C	XGB	XGB-C	XGB	XGB-C	XGB	XGB-C	XGB	XGB-C
1	0.738	0.741	0.218	0.199	0.725	0.704	0.170	0.166	0.675	0.713	0.213	0.226
2	0.747	0.723	0.240	0.243	0.756	0.746	0.226	0.197	0.723	0.703	0.260	0.276
3	0.691	0.663	0.321	0.323	0.659	0.660	0.269	0.267	0.706	0.723	0.289	0.285
4	0.753	0.822	0.226	0.221	0.752	0.814	0.200	0.187	0.689	0.819	0.247	0.264
5	0.757	0.848	0.204	0.207	0.730	0.822	0.200	0.190	0.774	0.834	0.201	0.222
6	0.766	0.842	0.263	0.246	0.737	0.849	0.217	0.193	0.773	0.859	0.268	0.260
7	0.769	0.877	0.212	0.208	0.776	0.881	0.184	0.184	0.784	0.886	0.205	0.233
8	0.690	0.726	0.242	0.260	0.725	0.718	0.220	0.209	0.666	0.630	0.273	0.294
9	0.732	0.728	0.239	0.235	0.738	0.755	0.214	0.202	0.727	0.731	0.258	0.253
10	0.734	0.750	0.310	0.326	0.696	0.740	0.227	0.243	0.732	0.750	0.287	0.303
11	0.708	0.811	0.256	0.218	0.723	0.811	0.246	0.208	0.663	0.776	0.265	0.236
12	0.775	0.880	0.224	0.235	0.781	0.852	0.208	0.201	0.740	0.845	0.250	0.260
13	0.797	0.853	0.217	0.225	0.741	0.859	0.209	0.186	0.786	0.846	0.206	0.245
14	0.806	0.894	0.243	0.206	0.747	0.885	0.237	0.187	0.761	0.879	0.274	0.234
15	0.780	0.933	0.196	0.179	0.786	0.922	0.161	0.142	0.770	0.927	0.214	0.209
16	0.790	0.909	0.261	0.211	0.765	0.899	0.232	0.193	0.768	0.893	0.249	0.230
17	0.858	0.950	0.145	0.141	0.842	0.943	0.152	0.132	0.862*	0.957 [¢]	0.134*	0.134^{ϕ}
18	0.790	0.941	0.201	0.180	0.786	0.935	0.192	0.138	0.752	0.935	0.228	0.197
19	0.866*	0.963 ^o	0.143*	0.136^{ϕ}	0.842*	0.954 ^o	0.146*	0.124¢	0.861	0.941	0.142	0.134
20	0.864	0.961	0.161	0.144	0.841	0.949	0.184	0.133	0.847	0.953	0.139	0.140
21	0.856	0.964*	0.150	0.135*	0.825	0.960*	0.161	0.119*	0.838	0.963*	0.148	0.130*
22	0.788	0.780	0.203	0.203	0.788	0.773	0.197	0.166	0.756	0.772	0.249	0.228

Note : *Best results, ϕ Second best results.



Conclusions

- The key insights drawn from the analyses can be summarized as :
 - The FPCA consistently outperforms the traditional PCA in terms of explanatory variance, when applied to time-dependent climate indexes.
 - The 4 principal components derived through FPCA are sufficiently effective in capturing the underlying patterns in crop yield variations.
 - The inclusion of indexes representing additional weather conditions such as wind speed, and sea-level changes alongside temperature and precipitation, significantly improves model performance.
 - The composite ACI index alone fails to fully capture and explain the complex weather conditions that affect crop yields.



References - I

- [1] ACI (2018). Actuaries Climate Index: Development and Design.
 American Academy of Actuaries, Canadian Institute of Actuaries,
 Casualty Actuarial Society, Society of Actuaries. For Version 1.1, April
 2019 see https://actuariesclimateindex.org/wp-content/
 uploads/2019/05/ACI.DevDes.2.20.pdf.
- [2] Chen, T. and Guestrin, C. (2016). Xgboost: A scalable tree boosting system. In *Proceedings of the 22nd acm sigkdd international conference on knowledge discovery and data mining*, pages 785–794.
- [3] CME Group (2024). https://www.cmegroup.com/markets/products.html.
- [4] Hotelling, H. (1933). Analysis of a complex of statistical variables into principal components. *Journal of Educational Psychology*, 24(6):417.
- [5] Jewson, S. and Brix, A. (2005). Weather derivative valuation: the meteorological, statistical, financial and mathematical foundations.

 Cambridge University Press.

References - II

- [6] Ke, G., Meng, Q., Finley, T., Wang, T., Chen, W., Ma, W., Ye, Q., and Liu, T.-Y. (2017). Lightgbm: A highly efficient gradient boosting decision tree. Advances in neural information processing systems, 30.
- [7] Massey Jr, F. J. (1951). The Kolmogorov–Smirnov test for goodness of fit. *Journal of the American Statistical Association*, 46(253):68–78.
- [8] Nelder, J. A. and Wedderburn, R. W. (1972). Generalized linear models. Journal of the Royal Statistical Society Series A: Statistics in Society, 135(3):370–384.
- [9] NOAA (2024). National Oceanic and Atmospheric Administration latitude/longitude distance calculator. https://www.nhc.noaa.gov/gccalc.shtml.
- [10] Odening, M., Mußhoff, O., and Xu, W. (2007). Analysis of rainfall derivatives using daily precipitation models: Opportunities and pitfalls. *Agricultural Finance Review*, 67(1):135.

References - III

- [11] Pearson, K. (1901). Liii. on lines and planes of closest fit to systems of points in space. The London, Edinburgh, and Dublin Philosophical Magazine and Journal of Science, 2(11):559–572.
- [12] Ramsay, J. O. and Silverman, B. W. (2002). *Applied functional data analysis: methods and case studies*. Springer.
- [13] Tibshirani, R. and Hastie, T. (1990). Generalized Additive Models, volume 43 of Monographs on Statistics and Applied Probability. Chapman and Hall/CRC.
- [14] USDA (2024). U.S. Department of Agriculture. https://www.usda.gov/.
- [15] Wood, S. N. (2017). Generalized Additive Models: An Introduction with R. Chapman and Hall/CRC, 2 edition.
- [16] Zar, J. H. (2005). Spearman Rank Correlation, chapter In Encyclopedia of Biostatistics (eds P. Armitage and T. Colton). John Wiley & Sons.

Thank you for your attention!

cyavrum@metu.edu.tr
skestel@metu.edu.tr
jose.garrido@concordia.ca



